J|A|C|S
COMMUNICATIONS

Published on Web 07/27/2007

Nanoparticle Synthesis via the Photochemical Polythiol Process

Scott C. Warren,[†,‡] Aaron C. Jackson,[‡] Zachary D. Cater-Cyker,[‡] Francis J. DiSalvo,[†] and Ulrich Wiesner*[,‡]

Department of Chemistry & Chemical Biology and Department of Materials Science & Engineering, Cornell University, Ithaca, New York 14853

Received May 11, 2007; E-mail: ubw1@cornell.edu

Significant quantities of waste are produced in the synthesis of metal nanoparticles. Charge-stabilized sols made by Faraday[1] and Turkevich[2] required 1 L of water to produce 40 and 60 mg of particles, respectively. Even ligand-stabilized particles, such as those made by the polyol process,[3] phase-transfer,[4] or reverse microemulsion,[5] use large quantities of ligands, surfactants, polymers, phase-transfer reagents, and solvents. As increasingly electropositive metals are fashioned into nanoparticles, stronger reducing agents are required. Not only are many of these reducing agents spontaneously flammable in air but their synthesis is energy intensive. Thus, "greener" methods of nanoparticle synthesis are needed.

Producing monodisperse nanoparticles of electropositive metals presents its own challenge. Because strong reducing agents must be employed, reduction of the metal salt occurs before the reducing agent can be distributed homogeneously through solution. Local variations in the rates of nucleation and growth result in polydisperse particles. To address this problem, strong reducing agents with slow kinetics are needed to enable homogeneous nucleation and growth. Such a class of slow but strong reducing agents may provide sufficient time for ligands to cap the growing nanoparticles, thereby allowing the relative strength of the ligand−nanoparticle interaction to slow[6] or stop[7] further growth. In this way, the production of monodisperse electropositive metal nanoparticles might be possible.

Biological systems provide a clue for solving this problem: peptides use the thiol/disulfide redox couple for controlling protein structure and function.[8] Thiols are remarkably strong reducing agents—depending on their structure, potentials as negative as −0.38 V vs SHE have been measured.[9] Compared to other reducing agents, thiols are moderately air-stable, safe, and inexpensive ($3.68/mole for dodecanethiol versus $9.36/mole for $NaBH_4$; see Supporting Information). Finally, because disulfides form monolayers on nanoparticle surfaces,[10] the thiol/disulfide can act as both the reducing agent and the stabilizing ligand.

A challenge with thiols results from their ability to form stable molecular compounds with many metal ions[11]—the resulting metal thiolate does not decompose further. To overcome this limitation, elevated temperature reduction/decomposition of Ag,[12] Bi,[13] and Te[14] has been employed to produce micron-sized aggregates or nanometer-thick platelets, sheets, or wires. Due to the ease with which metal sulfides are formed, however, thermal decomposition may not be broadly applicable.[15]

Here, we introduce the photochemical polythiol process (Scheme 1). In this process, the thiol reacts with a metal salt, generating a metal thiolate. This distributes the reducing agent homogeneously. Visible light then initiates a ligand-to-metal charge transfer (LMCT) in the metal thiolate, reducing the metal cation. This process was motivated by a UV-based decomposition of tin(II) dimethylamine to tin nanoparticles by Chaudret et al.[16] Here, we used the photochemical polythiol process to synthesize bismuth, copper, lead, and antimony nanoparticles (see Supporting Information). We focus on the room-temperature synthesis of rhombohedral bismuth nanoparticles with a narrow size distribution. Although bismuth nanoparticles have been previously described, the synthesis of monodisperse, homogeneous particles remains a challenge.[17−19]

Scheme 1. Synthetic Route for the Photochemical Polythiol Process (Metals Tested Include Bismuth, Copper, Antimony, and Lead)

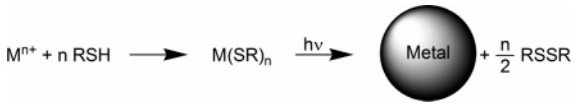

We used a bismuth(III) carboxylate such as acetate, 2-ethylhexanoate, or oleate as our bismuth source. In a typical synthesis, a 10 wt% solution of bismuth oleate in dry THF was prepared in a glass flask under N_2 (Figure 1A). Dodecanethiol was added to the bismuth oleate solution in a 3:1 molar ratio. The solution immediately turned yellow (ϵ = 2300 mol^{-1} cm^{-1} at 360 nm), indicating the formation of bismuth thiolate and oleic acid (Figures 1B, 3A, and UV−vis spectra, Supporting Information). Exposure to ambient light in our laboratory decomposed the bismuth thiolate, turning the solution black (Figure 1C). Continued irradiation at room temperature for 24 h (Figure 1D) or longer produced bismuth nanoparticles in high yield. Near-quantitative conversion to bismuth nanoparticles was achieved after 2 weeks. The solution was not stirred during the synthesis, allowing the nanoparticles to precipitate as colloidal crystals. This accelerated the rate of nanoparticle formation by minimizing photon absorption by the black bismuth nanoparticles. At the end of the synthesis, the solution was exposed to air and transferred to a centrifuge tube. The sample was centrifuged for 2 min at 9000 rpm. The colorless supernatant was removed, and the black solid was resuspended in THF by shaking the centrifuge tube. TEM grids were prepared from this solution, which contained a small amount of residual ligands. Centrifugation was repeated, and the black solid was dried at room temperature under vacuum to determine yield. Upon complete conversion, only 10 g of solvent was needed to produce 0.25 g of nanoparticles (78 wt% Bi). We achieved similar results when we applied the same protocol to other bismuth carboxylates.

Examination of the product by TEM reveals uniform rhombohedral nanoparticles (Figure 2A). Bismuth nanoparticles produced in this process are 9.2 ± 0.7 nm across (measured as the distance perpendicular to opposite faces). This degree of uniformity allows the nanoparticles to self-assemble into a superlattice that adopts the same symmetry as bismuth's rhombohedral atomic lattice (Figure 2C). Even after air exposure for several weeks, electron diffraction and HRTEM (Figure 2B,D) indicate the presence of crystalline bismuth. A 1−2 nm amorphous coating on the nanoparticles was observed, suggesting the formation of an oxide layer.

[†] Department of Chemistry & Chemical Biology.
[‡] Department of Materials Science & Engineering.

10.1021/ja0733639 CCC: $37.00

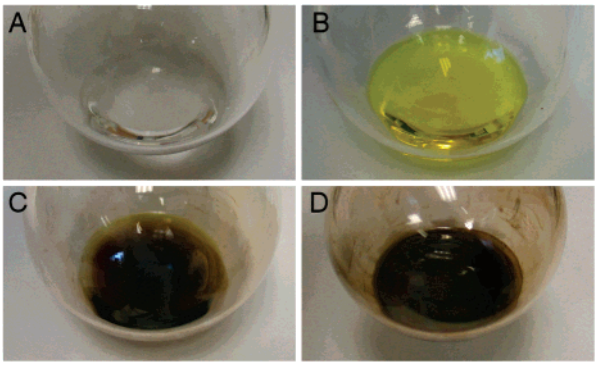

Figure 1. Photographs of nanoparticle synthesis. To a 10 wt% solution of bismuth oleate in THF (A) was added dodecanethiol, generating the yellow bismuth thiolate (B). The black color of nanoparticles is apparent after 2 h (C) and after 1 day (D) of exposure to ambient light.

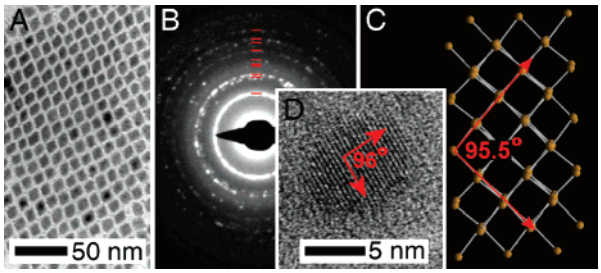

Figure 2. Superlattice of rhombohedral bismuth nanoparticles collected after 6 days of exposure to light (A) and corresponding electron diffraction in which red lines indicate the most intense expected reflections of bismuth (B). The unusual crystal structure of bismuth (C) can be observed in HRTEM (D).

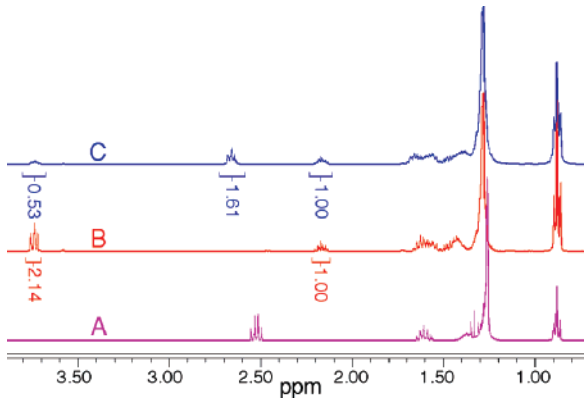

Figure 3. ^{1}H NMR of dodecanethiol (A), bismuth dodecanethiolate synthesized from bismuth 2-ethylhexanoate (B) and the same material after 4 days of irradiation at 365 nm (C). The synthesis was performed in a glass NMR tube in THF-d_8. Integrations are normalized to 2-ethylhexanoic acid's β-hydrogen (2.17 ppm).

We monitored the temporal evolution of bismuth nanoparticle formation by NMR (Figure 3). We found that the bismuth thiolate forms quantitatively within seconds, liberating the carboxylic acid (Figure 3 and Supporting Information). The CH_2 α to the thiol shifts from a doublet of triplets at 2.51 ppm (Figure 3A) to a triplet at 3.73 ppm (Figure 3B) upon formation of bismuth thiolate. After exposure to 365 nm light for 4 days at a power of 7 mW/cm^2, a decrease in the triplet at 3.73 ppm and growth of the triplet at 2.66 ppm (Figure 3C) indicated disulfide formation. Under these synthesis conditions, we achieved a 75% yield of nanoparticles after 4 days. As a control, an NMR tube of identically prepared bismuth dodecanethiolate kept in the dark for 4 days had a spectrum identical to that of Figure 3B, showing that no decomposition had occurred.

In summary, absorption of a photon initiates decomposition of a metal thiolate by a LMCT process. Because the reduction potential of the metals is more positive than that of the thiol, the resulting metal nanoparticles are not oxidized by the disulfide (see Figure S2, Supporting Information). The ability to reduce lead, which has a reduction potential of −0.125 V in acidic solution, demonstrates the possibility of reducing modestly electropositive elements. The photochemical polythiol process decomposes the metal thiolate in a slow, homogeneous process, affording uniform nanoparticles while using relatively small volumes of solvent.

The environmental benefits of this process can be extended through the use of sunlight to initiate the decomposition. Further experiments will examine the possibility of applying the photochemical polythiol process to other metals.

Acknowledgment. This work was supported by grants from the DOE (DE-FG02 87ER45298) and the NSF (DMR 0520404), through the Cornell Center for Materials Research. S.C.W. acknowledges support from the EPA's STAR fellowship program.

Supporting Information Available: Experimental procedures, characterization of new compounds, and discussion. This material is available free of charge via the Internet at http://pubs.acs.org.

References

(1) Faraday, M. *Philos. Trans. R. Soc.* **1857**, *147*, 145−181.
(2) Turkevitch, J.; Miner, R. S., Jr.; Babenkova, L. *J. Phys. Chem.* **1986**, *90*, 4765−4767.
(3) Blinov, I.; Balashev, K.; Shagisultanova, G. *Koord. Khim.* **1986**, *11*, 644.
(4) Brust, M.; Walker, M.; Bethell, D.; Schiffrin, D. J.; Whyman, R. *J. Chem. Soc., Chem. Commun.* **1994**, 801−802.
(5) Pileni, M. P. *Nat. Mater.* **2003**, *2*, 145−150.
(6) Niesz, K.; Grass, M.; Somorjai, G. A. *Nano Lett.* **2005**, *5*, 2238−2240.
(7) Zheng, N.; Fan, J.; Stucky, G. D. *J. Am. Chem. Soc.* **2006**, *128*, 6550−6551.
(8) Hiroshi, K.; Beckwith, J. *Nat. Cell Biol.* **2001**, *3*, E247−E249.
(9) Houk, J.; Whitesides, G. M. *J. Am. Chem. Soc.* **1987**, *109*, 6825−6836.
(10) Porter, L. A., Jr.; Ji, D.; Westcott, S. L.; Graupe, M.; Czernuszewicz, R. S.; Halas, N. J.; Lee, T. R. *Langmuir* **1998**, *14*, 7378−7386.
(11) Dance, I. G. *Polyhedron* **1986**, *5*, 1037−1104.
(12) Hu, X. L.; Zhu, Y. J. *Mater. Lett.* **2004**, *58*, 1517−1519.
(13) Chen, J.; Wu, L. M.; Chen, L. *Inorg. Chem.* **2007**, *46*, 586−591.
(14) Zhu, Y. J.; Hu, X. L. *Chem. Lett.* **2003**, *32*, 732−733.
(15) Larsen, T. H.; Sigman, M.; Ghezelbash, A.; Doty, R. C.; Korgel, B. A. *J. Am. Chem. Soc.* **2003**, *125*, 5638−5639.
(16) Soulantica, K.; Maisonnat, A.; Fromen, M.-C.; Casanove, M.-J.; Chaudret, B. *Angew. Chem., Int. Ed.* **2003**, *42*, 1945−1949.
(17) Fang, J.; Stokes, K. L.; Zhou, W. L.; Wang, W.; Lina, J. *Chem. Commun.* **2001**, 1872−1873.
(18) Wang, Y. W.; Hong, B. H.; Kim, K. S. *J. Phys. Chem. B* **2005**, *109*, 7067−7072.
(19) Yu, H.; Gibbons, P. C.; Kelton, K. F.; Buhro, W. E. *J. Am. Chem. Soc.* **2001**, *123*, 9198−9199.

JA0733639